*35th EPS Conference on Plasma Phys. Hersonissos, 9 - 13 June 2008 ECA Vol.**32D**, P-2.164 (2008)*

Diagnostics of ECR-MW Broad Beam Ion Sources

Holger Kersten[1*], Iulian Teliban[1], Viktor Schneider[1], Thomas Trottenberg[1],
Horst Neumann[2], Michael Tartz[2], Frank Scholze[2]
[1] *Institut für Experimentelle und Angewandte Physik, Christian-Albrechts-Universität, D-24098 Kiel, Germany*
[2] *Institut für Oberflächenmodifizierung, D-04318 Leipzig, Germany*

Introduction

Ion beam sources are widely used in material processing, especially for ion beam etching and ion beam assisted deposition [1, 2]. Using of ion beams for electric spacecraft propulsion is already applied and continuously improved [3, 4], e.g. SMART-1, DEEP SPACE-1. Knowledge about the beam properties, e.g. ion-energy distribution, ion-current density and their profiles, is necessary for all applications. Therefore, plenty of work has been spent in the improvement of ion sources [5, 6] and development of beam diagnostics.

In this paper we characterize the performance of an electron cyclotron resonance (ECR) microwave (MW) broad beam ion source [1] using different diagnostics. The beam properties such as density, energy and respective the profile are investigated using Faraday-cups and retarding-field analyzers. Axial and radial profiles of beam energy and density as functions of source parameters are measured. The results from different diagnostics are checked for consistency and discussed.

Experimental setup

A 50 l high vacuum (HV) stainless steel chamber is used for investigation of a broad beam ion source (IS, figure 1). The ECR ion source was developed by the Institut für Oberflächenmodifizierung Leipzig. The ion source and the chamber are vertically orientated to compensate the gravitational force by the ion beam for the later experiments which imply falling microparticles [5, 7]. The vacuum chamber was pumped down to a pressure of about 10^{-5} Pa by means of a turbomolecular pump backed by a scroll pump. The operation pressure is set to about $5*10^{-2}$ Pa by adjusting the process gas (argon) flow into the ion source. Due to the high transparency of the ion source grid system, the pressure in the ion source is only slightly higher than the chamber pressure.

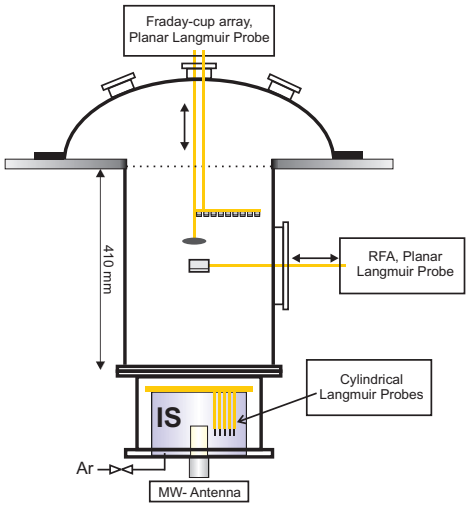

Figure 1: Schematic of the experimental set-up (VIBEX).

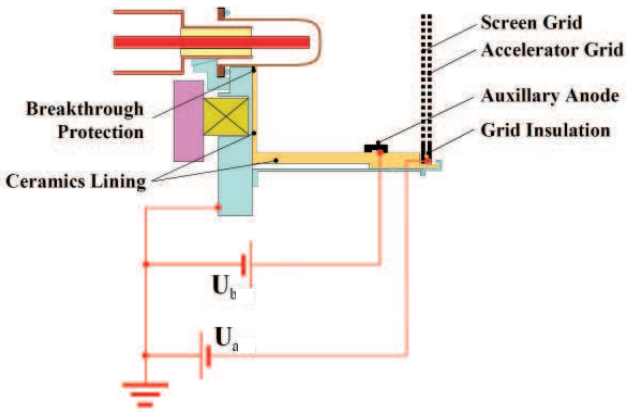

Figure 2: Schematic drawing of the IS discharge vessel and electrical circuits [6].

*email: kersten@physik.uni-kiel.de

Figure 2 shows a sketch of ion source and electrical circuits of the grids. An internal anode (*beam*) positively biased (U_b) is used to control the beam energy. The outer grid (*accelerator*) is negatively biased (U_a) and controls the beam density. The internal grid is used only for screening and is kept floating. Argon operation gas and a molybdenum grid system are used. The microwave power is set to 240 W for all measurements. Further details about ion source operation can be found elsewhere [1].

Ion beam diagnostic

The most important features of an ion source are the final beam properties. The electric potentials and currents at the source grids are deciding parameters for the beam density and ion energy [6]. Therefore, influence of the source parameters on the beam characteristics are analyzed in this section by means of the measured ion current density and ion-energy distribution function using Faraday-cups and retarding-field analyzers.

First, 1D ion beam profiles of the beam density are mapped using a Faraday-cup array consisting of nine analyzers (Figure 1), at different source parameters. Furthermore, by varying the axial distance from the grids, 2D maps of the broad beam are estimated. Figure 3 shows 2D profiles of the beam for different settings of the beam energy. The outer grid is grounded in the *no beam* case and kept at -100 V for other profiles. At the first glance these results show presence of a low density ion beam even for the grounded accelerator grid (*no beam*). This is caused by the ECR plasma potential (inside of the ion source) which is higher than 0 V. This setting is not used for the standard operation of the present ion source. It is analyzed only for a better understanding of the source plasma in the ion source.

For all profiles a rapid decay of the ion density with axial distance, i.e. about 50% in 10 cm, is observed. This is caused by the relatively high neutral gas pressure. The mean free path for Ar^+ is about 15 cm and is slightly increasing with the ion energy. On the other hand the beam width is similar to the source diameter (125 cm) close to the grids and only slightly broader far from the source. This indicates a self neutralization of the beam in our experiment.

In the radial direction the beam has a humped profile for high ion energies (600 eV, 800 eV) and presents a maximum at about 4 cm from the center. The profile is homogeneous in

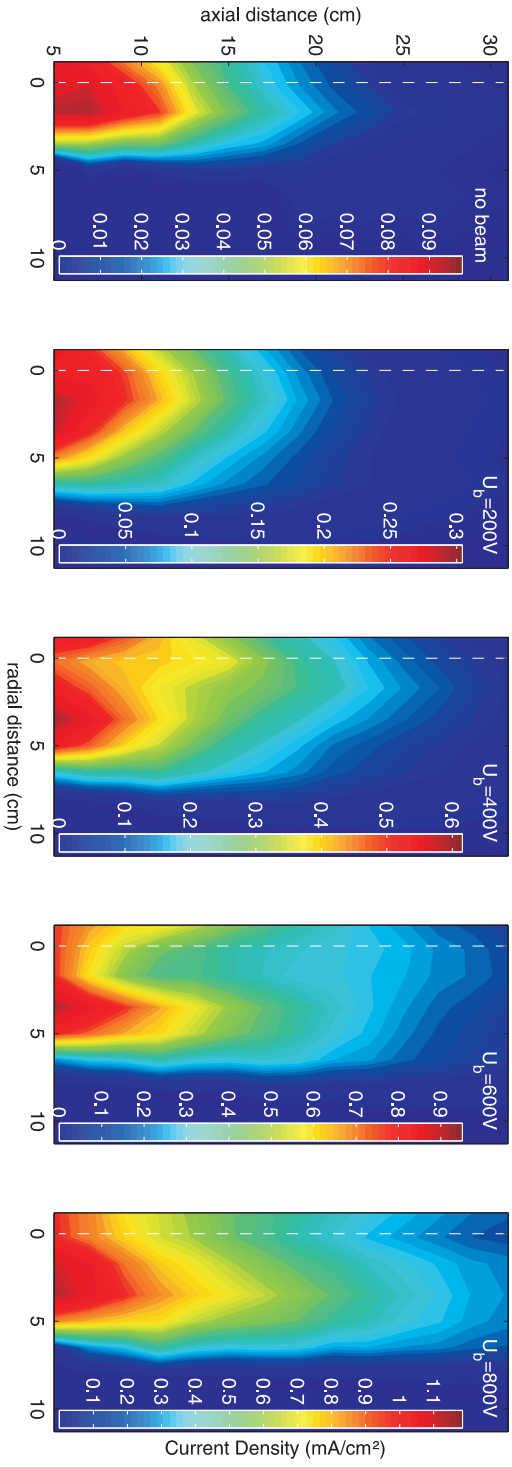

Figure 3: Ion density profiles for different beam energies. The white dotted line represents the source center. By the colorbar the current density scale is denoted.

azimuthal direction and is slightly shifted from the center of the source. That means, that the presence of the MW antenna (alumina cup) in the center of ECR plasma (Figure 2) influences the beam profile for high ion energies. The shift between the profile center and the principal axis (white dashed line) indicates that the focusing grids are not perfectly parallel.

Further on, the energy of the beam ions is carefully estimated using a three-grid retarding-field analyzer at 25 cm above the ion source. The analyzer carrier (see Figure 1) is moved to measure radial energy and density profiles.

Figure 4 shows the ion-energy distribution function (IEDF) for different beam energies. They are directly estimated from the first derivative of *I-V* analyzer characteristic. These profiles are acquired in the area of maximum current density, i.e. about 3 cm from the center (see Figure 3). The energy axis is normalized to the anode potential setting.

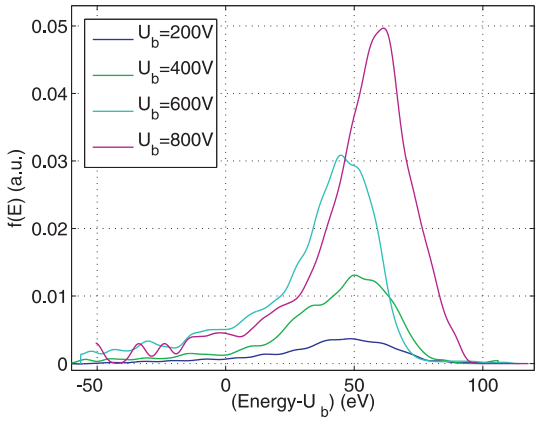

Figure 4: IEDF for different beam energies. The x-axis is normalized to the anode potential. Line color denotes the set ion energy as shown by the legend.

At the first view, IEDF show a maximum with about 50 eV above the set energy, i.e. anode potential. The shift indicates that ECR plasma potential is about (50-60) V above anode potential. On the other side the width of IEDF is slightly broader for low beam energy. It decreases from 45 eV at low beam energy (U_b=200 V) to 30 eV for energetic ions (U_b=800 V).

Figure 5 shows radial profiles of IEDF for different anode potentials. They indicate a similar width for all radial positions. The wrapper of IEDF profiles (red line) shows the radial density profiles at 25 cm above the ion source. The density units are arbitrary because the RFA transparency is not known and difficult to estimate because the repelling grids are not perfectly aligned. The density profile shape shows a good agreement with Faraday-cup array measurements (Figure 3).

Ion energy and density dependence on outer (*accelerator*) grid potential is further analyzed, too. Figure 6 shows IEDF profiles for different anode and accelerator potentials. This dependence shows a clear influence of the accelerator potential on the beam density. A gain in beam density of about 30% is obtained by increasing the accelerator potential by 200 V. On the other hand the beam energy is not influenced by the accelerator voltage. These

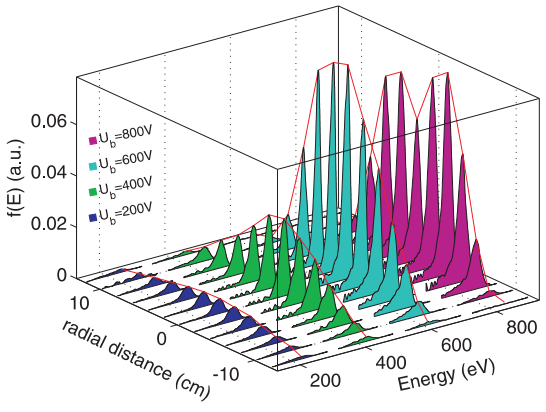

Figure 5: Radial IEDF profiles at different beam energies. The external read line is extrapolated from IEDF maximum for every radial position of the analyzer.

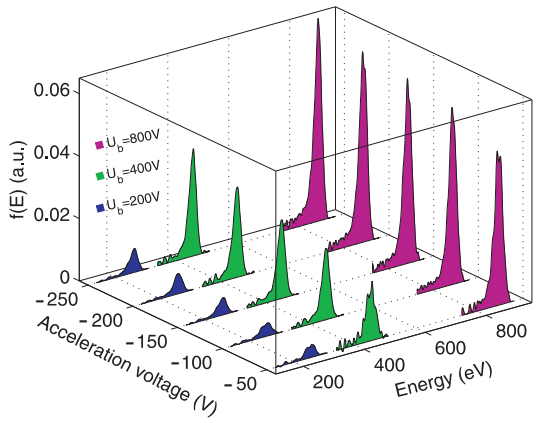

Figure 6: IEDF dependence on the accelerator potential. Colors indicate the corresponding anode potential.

results are in good agreement with previous measurements [6].

Summary

In this paper we have characterized the performance of an ECR/MW broad beam ion source according to beam density, ion energy distribution function and beam profile using electrical tools such as Faraday cups and retarding-field analyzers. 2D maps of the resulting beam profile have been measured using a Faraday-cup array. The beam profile generated by superposition of multiple beamlets, shows a humped shape which is slightly sifted according to the source center in case of high energetic beams. The beam diameter is similar to the source width even far from the grids. The beam width measurements indicate a self neutralization of the beam in our experiment. The ion energy was investigated using a three grid retarding-field analyzer. It shows a 50 eV above the set energy, i.e. by the anode potential, caused mainly by the ECR plasma potential. Therefore, the ECR plasma potential determines directly the ion beam energy although the plasma is controlled by the anode potential. Dependencies of beam energy and density on the source parameters have been carefully analyzed and confirm that the anode potential determines the beam energy and the grid voltage the beam-current density.

These investigations on beam energy, density and profile complete the previous experimental [5, 10] and theoretical [4, 8, 9] works. Furthermore, it is proved that relatively inexpensive tools can be used for diagnostics of broad ion beams.

Acknowledgment

The investigation on broad beam ion source is founded by the DLR project no. 50JR0643.

References

[1] M. Zeuner, F. Scholze, H. Neumann, T. Chasse, G. Otto, D.Roth, A. Hellmich, and B. Ocker, *Surface & Coatings Technology*, 142:11–20, 2001

[2] N. Sakudo, *Rev. Sci. Instrum.*, 71(2):1016–1022, 2000

[3] J. E. Pollard, and M. Martinez-Sanchez, *Journal of Prop. Power*, 14(5):688, 1998

[4] M. Tartz, E. Hartmann, R. Deltschew and H. Neumann, *Rev. Sci. Instrum.*, 71(2):732–734, 2000

[5] H. Kersten, R. Wiese, M. Hannemann, A. Kapitov, F. Scholze, H. Neumann, and R. Hippler, *Surface & Coatings Technology*, 200:809–813, 2005

[6] M. Zeuner, H. Neumann, F. Scholze, D. Flamm, M. Tartz, and F. Bigl, *Plasma Sources Sci. Technol.*, 7:252–268, 1998

[7] H. Kersten, R. Wiese, H. Neumann, and R Hippler, *Plasma Phys. Controlled Fusion*, 48:B105–B113, 2006

[8] M. Tartz, E. Hartmann, F. Scholze, and H. Neumann, *Rev. Sci. Instrum.*, 69(2):1147–1149, 1998

[9] J.H. Peters, M. Tartz, and H. Neumann, *Rev. Sci. Instrum.*, 77:03B, 2006

[10] M. Zeuner, J. Meichsner, H. Neumann, F. Scholze, and F. Bigl, *J. Appl. Phys.*, 80(2):611– 622, 1996